

Theory of Non-equilibrium “Hot” Carriers in Direct Band-gap Semiconductors Under Continuous Illumination

Subhajit Sarkar,^{*,†,‡} Ieng-Wai Un,[‡] Yonatan Sivan,[‡] and Yonatan Dubi^{†,¶}

[†]*Department of Chemistry, Ben-Gurion University of the Negev*

[‡]*School of Electrical and Computer Engineering, Ben-Gurion University of the Negev*

[¶]*Ilse Katz Center for Nanoscale Science and Technology, Ben-Gurion University of the
Negev*

E-mail: subhajit@post.bgu.ac.il, sbhjt72@gmail.com

October 26, 2021

Abstract

The interplay between the illuminated excitation of carriers and subsequent thermalization and recombination leads to the formation of non-equilibrium distributions for the “hot” carriers and to heating of both electrons, holes and phonons. In spite of the fundamental and practical importance of these processes, there is no theoretical framework which encompasses all of them and provides a clear prediction for the non-equilibrium carrier distributions. Here, a self-consistent theory accounting for the interplay between excitation, thermalization, and recombination in continuously-illuminated semiconductors is presented, enabling the calculation of non-equilibrium carrier distributions. We show that counter-intuitively, distributions deviate more from equilibrium under weak illumination than at high intensities. We mimic two experimental procedures to extract the carrier temperatures and show that they yield different dependence on illumination. Finally, we provide an accurate way to evaluate photoluminescence efficiency, which, unlike conventional models, predicts correctly the experimental results. These results provide a starting point towards examining how non-equilibrium features will affect properties hot-carrier based application.

1 Introduction

Illumination of semiconductors causes the generation of high energy non-thermal (aka “hot”) carriers (HCs)¹ which critically impacts the performance of semiconductor-based electronic and opto-electronic devices.²⁻⁴ Although the “hot” carrier (HC) dynamics in semiconductors have been studied for the past few decades,^{1,2} the topic has seen a growing interest in recent times due to technological relevance.^{3,5-8} Much experimental and theoretical efforts have been devoted to studying the *transient* dynamics of HCs in semiconductors under *ultrafast* pulsed illumination⁷⁻²⁰ with the aim of understanding the HC thermalization time scales and role of HC-phonon interaction that can affect performance of HC based solar energy conversion^{21,22} and lighting applications (e.g., photo-detection, HC based lasers).^{23,24}

Various key applications of semiconductors, such as solar-cells^{3,5,6,25-28} and lighting applications^{29,30} involve instead *continuous-wave* (CW) illumination, under which the system is necessarily in a non-equilibrium *steady-state* (NESS). The NESS consists of a carrier distribution that deviates from the thermal (i.e., Fermi-Dirac) distribution, and may also involve carrier temperatures differing from each other and from the lattice temperature.

Despite the extensive work on the topic, most studies involved only a macroscopic description of the problem, while the fewer existing state-of-the-art modelling of the NESS have several limitations. First, the tenet that the photo-excited HCs ultimately achieve the lattice temperature in the steady-state³¹ has been challenged in a recent experiment on group III-V semiconductors; it unveils that in the NESS carrier temperatures can be much higher than lattice temperature.³² A theoretical understanding of the existence of such a high carrier-temperature in NESS is still lacking,³² especially in light of the different techniques available for measuring the various temperatures. Second, the existing theoretical studies of the steady-state HC dynamics have considered the HC relaxation and interband recombination within the relaxation time approximation (RTA) where the scattering rate is assumed to be independent of the NESS distributions.³³⁻³⁶ Although the RTA makes the calculation of NESS distribution simpler, it neither conserves particle number nor energy within each band. Moreover, a constant (distribution-independent) relaxation rate may overestimate/underestimate the scattering rates, thereby misinterpreting the results. In addition, previous studies neglected the heating of the lattice,³⁷⁻³⁹ thus, they cannot treat correctly the amount of energy dissipated to the environment from the lattice, overall making it impossible to assess the difference between the carrier, phonon and environment temperatures. Last but not least, theoretical modelling of semiconductor photo-luminescence (PL) and cooling of SCs has been based on carrier-only (macroscopic) rate equations of the total number density (rather than the Fermi golden rule expression which relies on the energy distributions of electrons and holes),^{30,40-43} thus, neglecting the role of carrier-phonon interactions and system-environment coupling;⁴⁴⁻⁴⁷ this, again, leads to an inaccurate assessment of the lattice temperatures and even led to some debate in temperature measurements in optical cooling experiments.⁴⁸ The above list of approximations indicates the lack of a comprehensive theoretical approach that incorporates full non-equilibrium distributions in determining carrier excitation, recombination, and carrier scattering.

Motivated by the semiconductor applications perspective, the lack of a complete theory incorporating the non-equilibrium nature of the photo-excited carriers, and the advance in the theoretical formulation in metallic systems,⁴⁹ we put forward a theoretical formalism

for the non-equilibrium dynamics of HCs under CW illumination. In particular, we present a set of coupled Boltzmann-heat equations for the non-equilibrium photo-generated carrier distributions, whereby photo-excitation, carrier-carrier and carrier-phonon scattering rates, and recombination of electrons and holes are evaluated self-consistently within the Fermi golden rule, thus introducing (semi-) quantum behavior into the Boltzmann equation (BE). The macroscopic properties (e.g., the power flows and the phonon temperature) are obtained by integrating over the distributions and employing the conservation of particle number and energy for each subsystem.^{37–39} Incorporation of the full non-equilibrium distributions in a self-consistent way along with the energy and number conservation distinguishes our work from existing formalisms that treat the non-equilibrium only within RTA.^{33–39}

Counter-intuitively, we find the NESS carrier distribution is more out-of-equilibrium (i.e., less resembles an equilibrium distribution), indicating higher density of non-thermal carriers at low illumination intensities than at high intensities⁵⁰ due to inefficient thermalization at low intensities. Consequently, the temperatures of the carriers become ill-defined at low intensities, and depend on the way the temperatures are measured. We show this by extracting carrier temperatures using two generic experimental procedures frequently used, namely (i) extracting a temperature from the heat transfer between carriers and phonons (measured via, e.g., a floating thermal probe or a thermocouple^{51,52}), and (ii) by fitting the photoluminescence (PL) spectra.^{53–55} These two temperatures are shown to be very different from one another.

Finally, our formalism allows us to evaluate the energy partition for an illuminated semiconductor, i.e., how much of the power pumped into the system goes to heating-up the lattice, and how much remains in the “hot” electron sub-system and subsequently (partially) dissipates through radiative recombination. We show that this partition depends on the energy of the single photon but not on the total number of photons, and explain experimental observations of the PL efficiency in CW-illuminated Gallium Arsenide (GaAs).

2 Microscopic Formulation

To calculate the NESS carrier distributions $f_e(\mathcal{E})$ (for electrons) and $f_h(\mathcal{E})$ (for holes), while keeping the phonon subsystem in its own thermal equilibrium,⁴⁹ we use the semi-quantum Boltzmann equations (BEs),

$$\frac{\partial f_c(\mathcal{E}; T_{ph})}{\partial t} = \left(\frac{\partial f_c}{\partial t} \right)_{exc} + \left(\frac{\partial f_c}{\partial t} \right)_{rec} + \left(\frac{\partial f_c}{\partial t} \right)_{c-ph} + \left(\frac{\partial f_c}{\partial t} \right)_{c-c}, \quad (1)$$

where f_c be the electron distribution for $c = e$ in the conduction band, and hole distribution for $c = h$ in the valence band at an energy \mathcal{E} ; T_{ph} is the phonon temperature.

The right-hand-side of the BEs includes four central processes. The first is the photo-excitation process, which occurs upon absorption of a photon of energy $\hbar\omega$. The next process is the recombination of excited carriers by which photo-excited electrons and holes lose energy by emitting photons, a process known as PL. Third, the carrier-phonon ($c - ph$) interaction is responsible for transferring energy from the electrons and holes to the lattice. Last but not least, carrier-carrier scattering is responsible for thermalization of the electrons

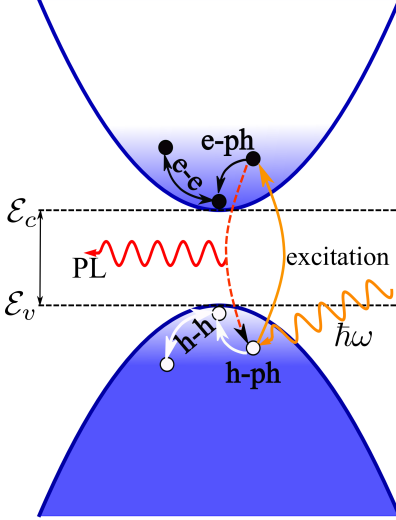


Figure 1: Schematic picture of the band structure of a representative semiconductor (GaAs) and the different processes participating in determining the non-equilibrium steady-state distributions. \mathcal{E}_c and \mathcal{E}_v are the energies of the conduction and valence band edges, respectively, and the chemical potential is placed at the middle of the band gap. Orange and red arrows denote photo-excitation and recombination (that leads to PL), respectively. e-e (h-h) solid black (white) arrow denotes carrier-carrier scattering and e-ph (h-ph) black (white) arrow denotes the carrier-phonon scattering.

and holes in their respective bands. Going forward, we explain and formulate these four processes in Sections 2.1-2.4. We neglect re-absorption of spontaneously emitted photons, Auger recombination and carrier-carrier Umklapp scattering, the reasons being explained in Sections 2.2, and 2.4, respectively.

2.1 Photo-excitation

The first term in Eq. (1), $(\frac{\partial f_c}{\partial t})_{exc}$, denotes the change in the population of carriers in the conduction and valence bands due to absorption of a photon of energy $\hbar\omega$, see Fig. 1. The formalism is based on the Fermi-golden rule energy-state based implementation for the case of metals^{49,56} but adapted to include the effect of the band-gap, i.e., the interband transitions; see Supplementary Section S1-A and S1-C for a detailed formulation.

In our formalism of the photo-excitation we do not explicitly incorporate momentum conservation, because in the presence of interactions of electrons and holes with phonons, defects and impurities present in the system, as well as for systems with finite size, the momentum is no longer a good quantum number. In this regard, for direct band gap SCs, our formulation of the photo-excitation process provides an upper bound for the number of excitation events (i.e., the maximum number of photo-excited carriers).

For indirect band-gap SCs, the interband transition due to photon absorption may require intraband carrier-phonon interaction to provide the necessary momentum transfer. This is because the conduction band minimum and the valence band maximum do not appear at the same \mathbf{k} -point in the Brillouin zone while an optical transition is associated with near-zero

momentum transfer. Moreover, any inter-valley (intraband optical) transition (for example, from the Γ -valley to L (or X)-valley) requires a direct intraband optical transition accompanied by a carrier-phonon and/or a carrier-carrier Umklapp scattering. Therefore, due to the absence of explicit momentum conservation our formulation of photo-excitation process can incorporate both indirect interband transitions and inter-valley (intraband) optical transitions only in the sense that it provides the upper bound for the number of excitation events. Nevertheless, for the intensities considered in this study, we explicitly show in Supplementary Section S1-A (equations S11 and S12) that any intraband optical transition is negligible compared to its interband counterpart. However, for even higher intensities and $\hbar\omega \sim \mathcal{E}_g$ intra-band optical transitions should be considered explicitly.

2.2 Recombination

The second term in Eq. (1), $(\frac{\partial f_c}{\partial t})_{rec}$, denotes the interband recombination of excited carriers, by which excited electrons and holes lose energy by spontaneously emitting photons leading to PL, see Fig. 1. We adopt the standard formulation, see Supplementary Sections S1-B and S1-D, for PL,^{33,57,58} which is also consistent with the formulation of the photo-excitation (Section 2.1) considered above. To this end, we relax the requirement of the momentum conservation for the same set of reasons corresponding to the photo-excitation process. Therefore, our formulation of recombination provides only an upper limit of the number of recombination events for indirect band-gap SCs.

Furthermore, we assume absorption of spontaneously emitted photons is a weak effect. Such an assumption is valid for systems with size smaller than the optical skin depth, such as nanoparticles and thin films. Most semiconductor applications, such as solar cells, lighting applications^{3,5,6,29,30,33} etc. meet this assumption. At this system size, the effective local electric field corresponding to the illumination is homogeneous throughout the system, and almost all the spontaneously emitted photons from inside the bulk of the system are radiated out of the system with a negligible fraction getting reabsorbed thus, justifying our assumption.

2.3 Carrier-phonon interaction

The electron-phonon ($e - ph$) and hole-phonon ($h - ph$) interactions (third term in Eq. (1)) are responsible for transferring energy from the electrons and holes to the lattice. These are schematically shown in Fig. 1. They occur within an energy window comparable to the Debye energy near the band edge (thus, it is typically narrow with respect to the photon energy). We consider the deformation potential approximation for the interaction between the carriers (both electrons and holes) and the phonons,¹⁸ where only the longitudinal acoustic phonons are taken into account; nevertheless, our formulation can be extended to incorporate optical phonons as well. Indeed, the Debye temperature (the corresponding Debye energy is $\hbar\omega_D = 0.024$ eV for GaAs) is comparable to room temperature, therefore, the higher energy optical phonon modes are expected to be less populated (e.g., optical phonon energy being $\hbar\omega_{ph} = 0.037$ eV in GaAs),¹⁹ and, thus, not considered here. Detailed formalism is given in Supplementary Section S2. Further support for the neglect of optical phonons is provided in

a recent study that showed that the “hot” electrons in GaAs lose energy chiefly by emitting acoustic phonons.¹³

2.4 Carrier-carrier interaction

The electron-electron interaction in the conduction band and hole-hole interaction in the valence band (fourth term in Eq. (1), altogether carrier-carrier scattering) are responsible for thermalization of the electrons and holes in their respective bands. This enables carriers to reach a quasi-equilibrium where a Fermi-Dirac distribution with a carrier temperature [$T_{e(h)}$ for electrons (holes)] can be associated to the carriers. Following Snoke *et al.*,¹⁸ we calculate the carrier-carrier scattering within the Fermi-Golden rule. The quantum nature of the carrier-carrier scattering comes from the Pauli exclusion principle incorporated into the distribution-dependent term, see equations (S32) and (S33). The carrier-carrier scattering rate depends on the density of (excited) carriers, and therefore, on the intensity of the incident light and the carrier temperature.^{59,60} For carrier densities $n_e < 10^{24} \text{ m}^{-3}$, the effect of Coulomb screening can be neglected as there are not much carriers to provide enough screening.^{59,61} We therefore, consider only hard sphere interactions between the carriers, see Supplementary Section S3. In most of the undoped III-V binary SCs with wider band-gaps [with exceptions being InSb ($\mathcal{E}_g = 0.235 \text{ eV}$), InAs ($\mathcal{E}_g = 0.417 \text{ eV}$) at room temperature] carrier density does not reach such high values for the illumination intensities considered in our study.^{59,61,62} Therefore, our formulation of carrier-carrier interaction applies to a large class of III-V binary SCs. For Ternary and Quaternary alloys energy band-gaps and room temperature carrier density strongly depend on the alloy composition,⁶³ and therefore, these are needed to be studied case by case.

Importantly, we discard Auger (non-radiative) recombination here, as it is negligible for the intensities we consider,^{42,64,65} and become appreciable only under extremely high carrier densities with spatial confinement (such as small nano-structures with system size even much less than that we already assumed in connection to absorption of the spontaneously emitted photons in Section 2.2) where spatial confinement can lead to a large overlap between electron and hole wave functions.⁶⁶ Moreover, we consider only pristine SCs, such that carrier-impurity scattering is neglected.⁶⁷

3 Macroscopic formulation - Energy and number conservation

Crucially, in order to account correctly for the non-equilibrium properties, energy conservation must be considered for each sub-system (electrons, holes and phonons) separately.⁴⁹ The rate of change of energy of the electronic subsystem (and analogously for holes) is obtained by integrating over the distribution functions (1) by $\int d\mathcal{E}(\mathcal{E} - \mathcal{E}_C) \left(\frac{\partial f_e}{\partial t}\right) \rho_e(\mathcal{E})$, \mathcal{E}_C being the energy of the conduction band edge $\left(\int d\mathcal{E}(\mathcal{E}_V - \mathcal{E}) \left(\frac{\partial f_h}{\partial t}\right) \rho_h(\mathcal{E})\right)$, \mathcal{E}_V being the energy of the

valence band edge) [see Fig. 1], resulting in

$$\frac{d\mathcal{U}_c}{dt} = W_{c-exc} - W_{c-rec} - W_{c-ph}, \quad (2)$$

where $\rho_c(\mathcal{E})$ is the carrier density of states (cDOS). We interpret equation (2) as the balance between the rate of gain of energy of the electronic (hole) subsystem due to the photo-excitation, viz., W_{c-exc} , the rate of loss of excess energy the electrons (holes) due to they recombination back to the conduction (valence) band, viz., W_{c-rec} , and the rate of energy flow to the lattice, W_{c-ph} . The elastic carrier-carrier scattering processes do not cause any change in the energy of the carrier subsystems, respectively. At the steady-state $\frac{d\mathcal{U}_c}{dt} = 0$ signifies the conservation of energy. See Supplementary Section S4 for more details.

Similarly, the total energy of the lattice, \mathcal{U}_{ph} , is balanced by the heat flowing in from the electron and hole subsystems and flowing out to the environment, viz.,

$$\frac{d\mathcal{U}_{ph}}{dt} = (W_{e-ph} + W_{h-ph}) - G_{ph-env}(T_{ph} - T_{amb}), \quad (3)$$

where G_{ph-env} is the coupling between the lattice and the environment, and is phenomenologically introduced in the formulation. See Supplementary Section S4 for further details. Moreover, value of G_{ph-env} may strongly depend on the geometry of the sample and on the thermal conductivity of the host.^{49,68}

We search numerically for a NESS based on the energy conservation, i.e., $\frac{d\mathcal{U}_e}{dt} = \frac{d\mathcal{U}_h}{dt} = \frac{d\mathcal{U}_{ph}}{dt} = 0$, when the semiconductor is maintained under CW illumination. When a steady-state is obtained, equations (1)-(3) provide us with the electron and hole distributions corresponding to the NESS, and the temperature of the lattice, T_{ph} . We then extract the steady-state electron and hole temperatures, T_e and T_h , respectively, by adapting two generic experimental procedures frequently used, (i) from the exchange of power between the electron (hole) sub-systems and the phonons (see Supplementary Section S6),^{51,52} and (ii) from the steady-state PL spectra (see Supplementary Section S7).⁵³⁻⁵⁵

4 Results

We take intrinsic (undoped) Gallium Arsenide (GaAs) as a specific material to understand and determine the non-equilibrium carrier distributions under CW illumination with varying intensities. However, our formulation can well be applied to pulsed-illumination with a suitable modification in the photo-excitation term $(\frac{\partial f_c}{\partial t})_{exc}$. Furthermore, although we consider the parabolic band dispersion [see Supplementary equation S1], we point out that our formulation is general enough to accommodate any dispersion relation since the cDOS is a function of energy either experimentally obtained or calculated from *ab-initio* density functional theory. The valence band edge, conduction band edge and the chemical potential are at $\mathcal{E}_V = 3.49$ eV, $\mathcal{E}_C = 4.91$ eV and $\mu = 4.2$ eV, respectively. The illumination photons have energy of $\hbar\omega = 1.65$ eV and the GaAs permittivity is set to $\epsilon''(\omega) = 3.3\epsilon_0$ at $\hbar\omega$,⁶⁹ where ϵ_0 is the free-space permittivity. Other parameters used in this study are given in supplementary Table S1 in Supplementary Section S5.

4.1 Non-equilibrium distribution:

FIG. 2(a) shows the steady-state distributions of holes f_h and electrons f_e as a function of the energy \mathcal{E} in the valence and conduction bands, respectively, for electric field levels ranging from $|E|^2 = 4(\text{V/m})^2$ [$1.976 \times 10^{-6} \text{ W/cm}^2$] to $|E|^2 = 4 \times 10^9(\text{V/m})^2$ [$1.976 \times 10^3 \text{ W/cm}^2$]. For comparison, we plot the thermal (Fermi-Dirac) distributions for electrons and holes f_e^T and f_h^T at ambient temperature.

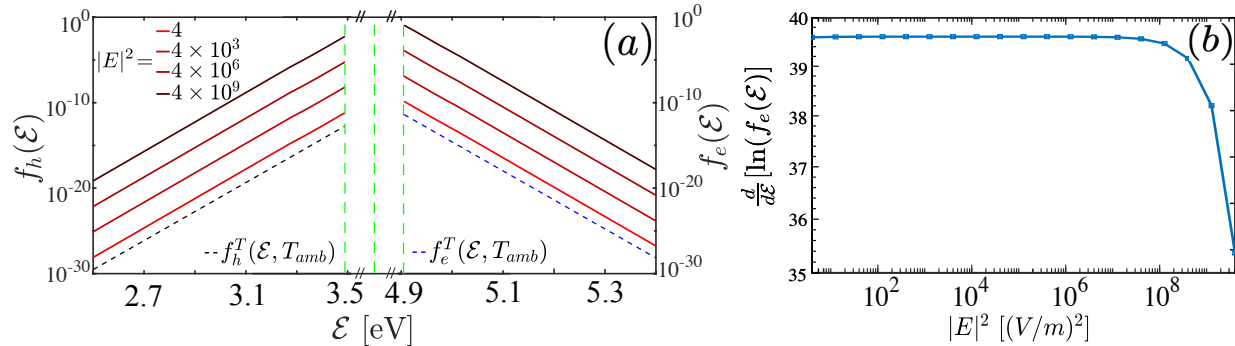


Figure 2: **Hole and the electron distributions:** (a) Plots of the hole distribution $f_h(\mathcal{E})$ in the valence band, the electron distributions $f_e(\mathcal{E})$ in the conduction band at different values of the local field. The valence band edge at \mathcal{E}_V , the conduction band edge at \mathcal{E}_C and the chemical potential μ are shown by green dashed vertical lines. The superscript T denotes the Fermi-Dirac distribution. (b) Plot of logarithmic slope of the non-equilibrium distribution of electrons $f_e(\mathcal{E})$ at electronic energy $\mathcal{E} = 4.914$ eV (an energy near the conduction band edge) as a function of local field $|E|^2$.

The population of the carriers increases with the illumination intensity while the (logarithmic) slopes of the steady-state distribution are nearly the same as that of the ambient thermal distribution at lower intensities. Since for a thermalized (i.e., Fermi-Dirac) distribution the slope is inversely proportional to the carrier temperature, an increase of the distribution without a change in slope is indicative of a non-thermal distribution. It is only at higher intensities, when $e-e$ and $h-h$ interactions become comparable to the $e(h)-ph$ coupling, that the slopes of $f_{e(h)}$ start to deviate from $f_{e(h)}^T(\mathcal{E}, T_{amb})$. To demonstrate this, in FIG. 2(b) we plot the slopes of $f_e(\mathcal{E})$ at $\mathcal{E} = 4.914$ eV (near the conduction band edge, where the strength of the $e-e$ interaction is the maximum and therefore, can affect $f_e(\mathcal{E})$ the most), as a function of the local field $|E|^2$. The slope of $f_e(\mathcal{E})$ remains unchanged, until the intensity reaches a critical value such that the $e-e$ interaction becomes comparable to the $e-ph$ interaction. This will also be reflected in the carrier temperature (see discussion below and Fig. 3(b)). Thus, at low intensities due to inefficient carrier-carrier interaction, the distributions are truly non-thermal, and only start to thermalize at higher illumination intensities.

4.2 Carrier temperatures

We now use the NESS distributions to extract macroscopic characteristics of interest. First, we extract (“effective”) electron and hole temperatures from the carrier-phonon power trans-

fers (see Supplementary Section S6). We denote ΔT_e and ΔT_h as the deviation of electron and hole temperatures, respectively, from the ambient temperature. These are plotted as a function of the local field in FIG. 3(a), showing a nonlinear increase with the illumination intensity by several hundreds of degrees. Such a nonlinear dependence stems from the fact that $W_{e(h)-ph}$ exhibits a nonlinear dependence on $T_{e(h)} - T_{ph}$. The difference between the values of ΔT_e and ΔT_h is due to the different effective band masses of electrons and holes, and the different deformation potentials in the conduction and valence bands, see supplementary Table S1.

FIG. 3(b) shows the rise in the carrier temperature above ambient, denoted by ΔT_c , extracted from the PL (see Supplementary Section S7), as a function of the local field. It is worth emphasizing that the rise in electron and hole temperatures, obtained from the PL spectra is the same, because the recombination process that gives rise to PL is symmetric with respect to electrons and holes. ΔT_c exhibits a nonlinear increase with the intensity, and differs considerably from $\Delta T_{e(h)}$ both qualitatively and quantitatively throughout the entire range of the local fields. In particular, T_c obtained from the PL spectra deviate 5 – 15 K from T_{amb} which is much smaller compared to the deviation of $T_{e(h)}$ from T_{amb} obtained from carrier-phonon power transfers. However, as explained above, with increasing intensity, thermalization becomes more important, especially above a critical intensity (corresponding to a carrier density $n_e \approx 5.2 \times 10^{19} \text{ m}^{-3}$ here). The value of ΔT_c starts increasing above this critical intensity indicating the role of thermalization in a PL-based temperature measurement. This is also evident from the similarity between FIG. 3(b) and FIG. 2(b).

In FIG. 3(c) we plot the increase in phonon (lattice) temperature from the ambient, ΔT_{ph} , as a function of the local field, showing a linear dependence on the square of the local electric field. The total power transferred to the lattice from both electron and hole sub-systems exhibits the same linear dependence on the square of the local field (not shown). At the steady-state we find that $\Delta T_{ph} = (W_{e-ph} + W_{h-ph})/G_{ph-env}$, explaining the linear dependence of ΔT_{ph} on $|E|^2$, see Eq. (3). The tiny increase in T_{ph} with respect to the ambient temperature implies that the lattice hardly heats up at all. However, since $\Delta T_{ph} \propto G_{ph-env}^{-1}$, weaker lattice-environment coupling would lead to more heating of the lattice and vice versa. Interestingly, in the case of metals, electron-phonon coupling G_{e-ph} was orders of magnitude higher due to the larger number of electrons, and even exceeded G_{ph-env} .⁴⁹ In that sense, while the bottleneck of the energy flow in metals was the heat transfer from the phonons to the environment, for semiconductors, the bottleneck is the $e(h) - ph$ coupling.

4.3 Energy partition and efficiency

Our formulation provides a unique prediction for the partition between the two channels by which the electron/hole sub-system dissipates its energy, viz., interband recombination and energy transfer to the lattice via phonons. This is crucial for the correct prediction of semiconductor heating and associated photo-thermal nonlinearity in SC nanostructures (for example, recently studied in Silicon nanostructures; notably an indirect band-gap SC),^{70,71} quantification of the strength of PL, applications relying on these quantities such as thermometry and imaging, and most importantly, lighting applications of semiconductors.^{29,72,73}

Thus, we define $\eta_{rec}^{(c)} = W_{c-rec}/W_{c-exc}$ as the ratio of the power dissipated from the electron/hole sub-systems through recombination W_{c-rec} to the power absorbed by the elec-

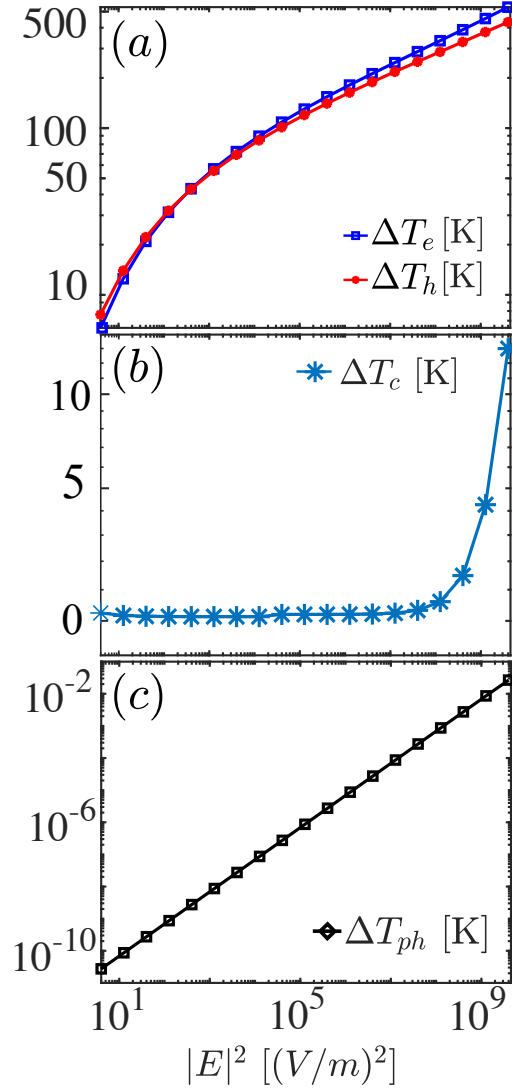


Figure 3: **Temperatures and energy partitions:** (a) The plot of $\Delta T_e = T_e - T_{\text{amb}}$ and $\Delta T_h = T_h - T_{\text{amb}}$ corresponding to the rise in the electron and hole temperatures, respectively, from the ambient temperature as a function of the local field $|E|^2$, in the units of $(V/m)^2$, on a log-log scale obtained from $e - ph$ interaction. (b) The plot of $\Delta T_c = T_c - T_{\text{amb}}$ carrier temperatures from the ambient temperature as a function of $|E|^2$, in the units of $(V/m)^2$, on a log-log scale obtained from fitting the PL spectra, with a 95% fitting accuracy. (c) The plot of $\Delta T_{ph} = T_{ph} - T_{\text{amb}}$ the rise in phonon temperature from the ambient temperature, indicating the lattice heating, as a function of $|E|^2$ on a log-log scale. The values of ΔT_{ph} indicates that the lattice does not heat up at all.

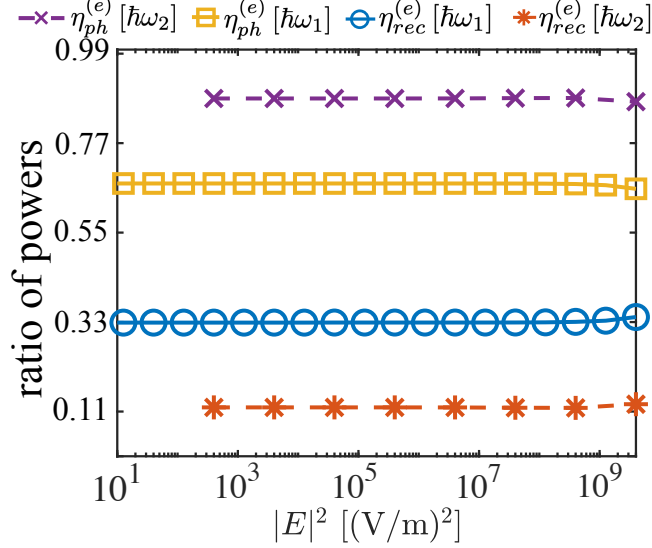


Figure 4: **Energy partitions:** The ratios $\eta_{rec}^{(e)}$ (blue circles and red stars) and $\eta_{ph}^{(e)}$ (yellow square and magenta cross) (see text definitions) corresponding to the photon energies $\hbar\omega = 1.65$ eV (yellow and blue solid lines, respectively) and 2.05 eV (magenta and red dashed lines, respectively), respectively, as a function of $|E|^2$ on a semi-log scale.

tron/hole sub-systems, W_{c-exc} ; similarly, $\eta_{ph}^{(c)} = W_{c-ph}/W_{c-exc}[\approx (1 - \eta_{rec}^{(c)})]$ as the ratio between the power transferred from the electron/hole sub-systems to the phonons, W_{c-ph} , and the power absorbed by the electron/hole sub-systems. FIG. 4 shows $\eta_{rec}^{(e)}$ and $\eta_{ph}^{(e)}$ for two different photon energies 1.65 and 2.05 eV ($\eta_{rec}^{(h)}$ and $\eta_{ph}^{(h)}$ are quantitatively the same as that of the electrons). We note that the energy partition is inversely proportional to the photon energy, i.e., $\eta_{rec}^{(c)} \propto (\hbar\omega - \mathcal{E}_g)^{-1}$, but does not depend on intensity, see Fig. 4. The reason is rather straightforward; for higher photon energies, electrons cross the energy gap to higher energies in the conduction band. They, thus, have more energy to lose to phonons before reaching the band edge and recombining.

Most importantly, the energy partitions can also be used to evaluate the efficiency of the PL process. The total power absorbed W_{abs} by the system is $\hbar\omega N_{exc}$, where N_{exc} is the rate of photon absorption per unit volume, and the total power lost due to PL is $W_{PL} = W_{e-rec} + W_{h-rec} + \mathcal{E}_g N_{exc}$ (note that $N_{exc} = N_{rec}$, the rate of recombination being equal to the rate of excitation at the steady-state, as required by the particle number conservation). The efficiency of the PL process is then obtained to be [see Supplementary Section S8],

$$\eta_{PL}^{QE} = \frac{W_{PL}}{W_{abs}} = \frac{\eta_{rec}^{(e)} + \eta_{rec}^{(h)}}{2} + \frac{\mathcal{E}_g}{\hbar\omega} \left[1 - \frac{\eta_{rec}^{(e)} + \eta_{rec}^{(h)}}{2} \right]. \quad (4)$$

For the example we study here, we find the efficiency η_{PL}^{QE} to be 90.6% and 73% at photon energies 1.65 and 2.05 eV, respectively. We compare this to experimental observations,⁴² where the PL efficiency was measured as a function of illumination intensity (under laser

light of 633nm). In these experiments, the low-intensity regime is dominated by trap-assisted recombination (e.g., Shockley-Read-Hall recombination), an effect which we do not account for. At high intensities interband recombination is dominant, and the PL efficiency saturates at around 71% (obtained by interpolating the experimental data), very close to our theoretical result, showing that the saturation of efficiency comes due to the phonon-mediated dissipation of carrier energy.

It is worth emphasizing again that although existing formulations for evaluation of PL efficiency account for trap-assisted and Auger recombination,^{30,40–43} these are macroscopic formulations based on (rate equations of) carrier density instead of carrier distribution and ignore the role of phonons. This prevents these formulations from being able to explain the high intensity PL efficiency. Put simply, without considering carrier-phonon interactions, PL efficiency should reach 100% at high intensities, which is in contradiction to experimental observations. Our theory thus provides a much improved theoretical prediction for PL efficiency. Moreover, our theory may also serve as a basis for a more rigorous microscopic formulation (in terms of carrier distribution f_c) of laser cooling of semiconductors,⁴⁷ and can allow the quantification of the possible role of carrier-phonon scattering as a heating path-way that hinders cooling.⁴⁸

5 Conclusions and discussion

In conclusion, we employed a semi-quantum BE formulation (including, importantly, energy and particle number conservation), to study the full non-equilibrium carrier distributions and temperatures in an SC under continuous illumination, taking GaAs as a specific example. Our formalism can easily be applied to all the direct band-gap semiconductors, and for indirect semiconductors, it can provide an upper limit of the full non-equilibrium carrier distributions and temperatures. Under low intensity illumination, we find that thermalization processes are inefficient, and the system remains at strong non-equilibrium. Somewhat surprisingly, for high intensities the SC tends to thermalize more efficiently due to increased carrier-carrier interaction at increased particle number densities. Although the lack of thermalization of the “hot” (non-thermal) carriers leaves room for the use of “hot” carrier-based SC electronics, how much the (more efficient) thermalization (at even higher intensities than considered here) can limit the use of “hot” carriers remains to be determined. Our theoretical formulation serves as a first step towards such a quantitative estimation.

Our formulation also allowed us to evaluate carrier temperatures in two ways, corresponding to two different experimental techniques, namely (i) through carrier-phonon energy transfer (measured via, e.g., a floating thermal probe or a thermocouple^{51,52}), and (ii) photoluminescence-based carrier temperature. We find that these two values deviate substantially from each other, again indicating strong non-equilibrium, and providing direct experimental predictions to test our theory.

Finally, our formulation provides a simple way to evaluate the PL efficiency, which is found to compare remarkably well with experimental observations and goes beyond existing theoretical models.^{30,40–43} Our model can be used as a theoretical platform to study outstanding open questions in the field, for instance, the persistent long-lived non-thermal carriers and the increase in carrier temperature recently observed in GaAs and other III-V semi-

conductors under CW illumination,³² and may enable the clarification of the controversial issues related to optical cooling and temperature of SCs.⁴⁸ Our formalism can be extended to other non-equilibrium situations, such as current-carrying junctions, doped semiconductors, and be used to evaluate and optimize the PL efficiency of, e.g., HC solar cells,^{3,5,6} optical cooling,^{42,47,74} and many other light emitting devices.^{29,30}

Supporting Information

Carrier-Photon Interaction: Photo-Excitation And Recombination. Carrier-Phonon Interaction. Carrier-Carrier Interaction. Parameters Of Intrinsic Gallium Arsenide. Conservation Of Energy And Number Of Particles. Extraction Of T_e And T_h From $W_c - ph^T$. Steady-State Photo-Luminescence. Efficiency Of The Photo-Luminescence Process.

Acknowledgements:

IWU and YS were supported by Israel Science Foundation (ISF) grant (340/2020) and by Lower Saxony - Israel cooperation grant no. 76251-99-7/20 (ZN 3637).

References

- (1) Shah, J. In *Hot Carriers in Semiconductor Nanostructures*; Shah, J., Ed.; Academic Press: San Diego, 1992; pp 3 – 14.
- (2) Takeda, E.; Suzuki, N. An empirical model for device degradation due to hot-carrier injection. *IEEE Electron Device Letters* **1983**, *4*, 111–113.
- (3) Green, M. A.; Bremner, S. P. Energy conversion approaches and materials for high-efficiency photovoltaics. *Nature Materials* **2017**, *16*, 23–34.
- (4) Nozik, A. J. Utilizing hot electrons. *Nature Energy* **2018**, *3*, 170–171.
- (5) König, D.; Casalenuovo, K.; Takeda, Y.; Conibeer, G.; Guillemoles, J.; Patterson, R.; Huang, L.; Green, M. Hot carrier solar cells: Principles, materials and design. *Physica E: Low-dimensional Systems and Nanostructures* **2010**, *42*, 2862 – 2866, 14th International Conference on Modulated Semiconductor Structures.
- (6) Conibeer, G.; Ekins-Daukes, N.; Guillemoles, J.-F.; König, D.; Cho, E.-C.; Jiang, C.-W.; Shrestha, S.; Green, M. Progress on hot carrier cells. *Solar Energy Materials and Solar Cells* **2009**, *93*, 713 – 719, 17th International Photovoltaic Science and Engineering Conference.
- (7) Rossi, F.; Kuhn, T. Theory of ultrafast phenomena in photoexcited semiconductors. *Rev. Mod. Phys.* **2002**, *74*, 895–950.

- (8) Sjakste, J.; Tanimura, K.; Barbarino, G.; Perfetti, L.; Vast, N. Hot electron relaxation dynamics in semiconductors: assessing the strength of the electron–phonon coupling from the theoretical and experimental viewpoints. *Journal of Physics: Condensed Matter* **2018**, *30*, 353001.
- (9) Shah, J. In *Hot Carriers in Semiconductor Nanostructures*; Shah, J., Ed.; Academic Press: San Diego, 1992; pp 279 – 312.
- (10) Elsaesser, T.; Shah, J.; Rota, L.; Lugli, P. Initial thermalization of photoexcited carriers in GaAs studied by femtosecond luminescence spectroscopy. *Physical review letters* **1991**, *66*, 1757.
- (11) Schoenlein, R.; Lin, W.; Ippen, E.; Fujimoto, J. Femtosecond hot-carrier energy relaxation in GaAs. *Applied Physics Letters* **1987**, *51*, 1442–1444.
- (12) Doany, F. E.; Grischkowsky, D. Measurement of ultrafast hot-carrier relaxation in silicon by thin-film-enhanced, time-resolved reflectivity. *Applied Physics Letters* **1988**, *52*, 36–38.
- (13) Bernardi, M.; Vigil-Fowler, D.; Ong, C. S.; Neaton, J. B.; Louie, S. G. Ab initio study of hot electrons in GaAs. *Proceedings of the National Academy of Sciences* **2015**, *112*, 5291–5296.
- (14) Selbmann, P. E.; Gulia, M.; Rossi, F.; Molinari, E.; Lugli, P. Coupled free-carrier and exciton relaxation in optically excited semiconductors. *Phys. Rev. B* **1996**, *54*, 4660–4673.
- (15) Goodnick, S. M.; Lugli, P. In *Hot Carriers in Semiconductor Nanostructures*; Shah, J., Ed.; Academic Press: San Diego, 1992; pp 191 – 234.
- (16) Fischetti, M. V.; Laux, S. E. Monte Carlo analysis of electron transport in small semiconductor devices including band-structure and space-charge effects. *Physical Review B* **1988**, *38*, 9721.
- (17) Jacoboni, C.; Reggiani, L. The Monte Carlo method for the solution of charge transport in semiconductors with applications to covalent materials. *Reviews of Modern Physics* **1983**, *55*, 645.
- (18) Snoke, D. W.; Rühle, W. W.; Lu, Y.-C.; Bauser, E. Evolution of a nonthermal electron energy distribution in GaAs. *Phys. Rev. B* **1992**, *45*, 10979–10989.
- (19) Sjakste, J.; Vast, N.; Barbarino, G.; Calandra, M.; Mauri, F.; Kanasaki, J.; Tanimura, H.; Tanimura, K. Energy relaxation mechanism of hot-electron ensembles in GaAs: Theoretical and experimental study of its temperature dependence. *Phys. Rev. B* **2018**, *97*, 064302.
- (20) Wittenbecher, L.; Viñas Boström, E.; Vogelsang, J.; Lehman, S.; Dick, K. A.; Verdozzi, C.; Zigmantas, D.; Mikkelsen, A. Unraveling the Ultrafast Hot Electron Dynamics in Semiconductor Nanowires. *ACS Nano* **2021**, *15*, 1133–1144.

- (21) Ferry, D. In search of a true hot carrier solar cell. *Semiconductor Science and Technology* **2019**, *34*, 044001.
- (22) Esmailpour, H.; Dorman, K. R.; Ferry, D. K.; Mishima, T. D.; Santos, M. B.; Whiteside, V. R.; Sellers, I. R. Exploiting intervalley scattering to harness hot carriers in III–V solar cells. *Nature Energy* **2020**, *5*, 336–343.
- (23) Lao, Y.-F.; Perera, A. G. U.; Li, L. H.; Khanna, S. P.; Linfield, E. H.; Liu, H. C. Tunable hot-carrier photodetection beyond the bandgap spectral limit. *Nature Photonics* **2014**, *8*, 412–418.
- (24) Elsässer, M.; Hense, S. G.; Wegener, M. Subpicosecond switch-off and switch-on of a semiconductor laser due to transient hot carrier effects. *Applied Physics Letters* **1997**, *70*, 853–855.
- (25) Polman, A.; Atwater, H. A. Photonic design principles for ultrahigh-efficiency photovoltaics. *Nature Materials* **2012**, *11*, 174–177.
- (26) Hirst, L. C.; Walters, R. J.; Führer, M. F.; Ekins-Daukes, N. J. Experimental demonstration of hot-carrier photo-current in an InGaAs quantum well solar cell. *Applied Physics Letters* **2014**, *104*, 231115.
- (27) Rodière, J.; Lombez, L.; Le Corre, A.; Durand, O.; Guillemoles, J.-F. Experimental evidence of hot carriers solar cell operation in multi-quantum wells heterostructures. *Applied Physics Letters* **2015**, *106*, 183901.
- (28) Ašmontas, S.; Gradauskas, J.; Sužiedėlis, A.; Šilėnas, A.; Širmulis, E.; Švedas, V.; Vaičiškauskas, V.; Žalys, O. Hot carrier impact on photovoltage formation in solar cells. *Applied Physics Letters* **2018**, *113*, 071103.
- (29) Li, J.; Zhang, G. Q. *Light-Emitting Diodes: Materials, Processes, Devices and Applications*; Springer, 2019.
- (30) Li, S. S. In *Semiconductor Physical Electronics*; Li, S. S., Ed.; Springer New York: New York, NY, 2006; pp 458–512.
- (31) Nozik, A. J. SPECTROSCOPY AND HOT ELECTRON RELAXATION DYNAMICS IN SEMICONDUCTOR QUANTUM WELLS AND QUANTUM DOTS. *Annual Review of Physical Chemistry* **2001**, *52*, 193–231, PMID: 11326064.
- (32) Tedeschi, D.; De Luca, M.; Fonseka, H. A.; Gao, Q.; Mura, F.; Tan, H. H.; Rubini, S.; Martelli, F.; Jagadish, C.; Capizzi, M.; Polimeni, A. Long-Lived Hot Carriers in III–V Nanowires. *Nano Letters* **2016**, *16*, 3085–3093.
- (33) Kamide, K.; Mochizuki, T.; Akiyama, H.; Takato, H. Nonequilibrium Theory of the Conversion Efficiency Limit of Solar Cells Including Thermalization and Extraction of Carriers. *Phys. Rev. Applied* **2018**, *10*, 044069.

- (34) Takeda, Y.; Motohiro, T.; König, D.; Aliberti, P.; Feng, Y.; Shrestha, S.; Conibeer, G. Practical Factors Lowering Conversion Efficiency of Hot Carrier Solar Cells. *Applied Physics Express* **2010**, *3*, 104301.
- (35) Kamide, K. Current–voltage curves and operational stability in hot-carrier solar cell. *Journal of Applied Physics* **2020**, *127*, 183102.
- (36) König, D.; Yao, Y.; Puthen-Veettil, B.; Smith, S. C. Non-equilibrium dynamics, materials and structures for hot carrier solar cells: a detailed review. *Semiconductor Science and Technology* **2020**, *35*, 073002.
- (37) Dimmock, J. A. R.; Day, S.; Kauer, M.; Smith, K.; Heffernan, J. Demonstration of a hot-carrier photovoltaic cell. *Progress in Photovoltaics: Research and Applications* **2014**, *22*, 151–160.
- (38) Tsai, C.-Y. Theoretical model and simulation of carrier heating with effects of nonequilibrium hot phonons in semiconductor photovoltaic devices. *Progress in Photovoltaics: Research and Applications* **2018**, *26*, 808–824.
- (39) Tsai, C.-Y. The effects of intraband and interband carrier-carrier scattering on hot-carrier solar cells: A theoretical study of spectral hole burning, electron-hole energy transfer, Auger recombination, and impact ionization generation. *Progress in Photovoltaics: Research and Applications* **2019**, *27*, 433–452.
- (40) Hall, R. N. Electron-Hole Recombination in Germanium. *Phys. Rev.* **1952**, *87*, 387–387.
- (41) Shockley, W.; Read, W. T. Statistics of the Recombinations of Holes and Electrons. *Phys. Rev.* **1952**, *87*, 835–842.
- (42) Johnson, S. R.; Ding, D.; Wang, J.-B.; Yu, S.-Q.; Zhang, Y.-H. Excitation dependent photoluminescence measurements of the nonradiative lifetime and quantum efficiency in GaAs. *Journal of Vacuum Science & Technology B: Microelectronics and Nanometer Structures Processing, Measurement, and Phenomena* **2007**, *25*, 1077–1082.
- (43) Chuang, S. *Physics of Photonic Devices*; Wiley Series in Pure and Applied Optics; Wiley, 2009; Chapter 2,9,10.
- (44) Hess, O.; Kuhn, T. Maxwell-Bloch equations for spatially inhomogeneous semiconductor lasers. I. Theoretical formulation. *Phys. Rev. A* **1996**, *54*, 3347–3359.
- (45) Hannewald, K.; Glutsch, S.; Bechstedt, F. Theory of photoluminescence in semiconductors. *Phys. Rev. B* **2000**, *62*, 4519–4525.
- (46) Hannewald, K.; Glutsch, S.; Bechstedt, F. Nonequilibrium photoluminescence excitation spectroscopy in GaAs: Bottleneck and memory effects. *Phys. Rev. B* **2003**, *67*, 233202.
- (47) Sheik-Bahae, M.; Epstein, R. I. Can Laser Light Cool Semiconductors? *Phys. Rev. Lett.* **2004**, *92*, 247403.

- (48) Morozov, Y. V.; Zhang, S.; Pant, A.; Jankó, B.; Melgaard, S. D.; Bender, D. A.; Pauzauskis, P. J.; Kuno, M. Can lasers really refrigerate CdS nanobelts? *Nature* **2019**, *570*, E60–E61.
- (49) Dubi, Y.; Sivan, Y. “Hot” electrons in metallic nanostructures—non-thermal carriers or heating? *Light: Science & Applications* **2019**, *8*, 89.
- (50) Neges, M.; Schwarzburg, K.; Willig, F. Monte Carlo simulation of energy loss and collection of hot charge carriers, first step towards a more realistic hot-carrier solar energy converter. *Solar Energy Materials and Solar Cells* **2006**, *90*, 2107 – 2128.
- (51) Dubi, Y.; Di Ventra, M. Colloquium: Heat flow and thermoelectricity in atomic and molecular junctions. *Reviews of Modern Physics* **2011**, *83*, 131.
- (52) Cui, L.; Jeong, W.; Fernández-Hurtado, V.; Feist, J.; García-Vidal, F. J.; Cuevas, J. C.; Meyhofer, E.; Reddy, P. Study of radiative heat transfer in Ångström- and nanometre-sized gaps. *Nature communications* **2017**, *8*, 1–9.
- (53) Hirst, L. C.; Walters, R. J.; Führer, M. F.; Ekins-Daukes, N. J. Experimental demonstration of hot-carrier photo-current in an InGaAs quantum well solar cell. *Applied Physics Letters* **2014**, *104*, 231115.
- (54) Nguyen, D.-T.; Lombez, L.; Gibelli, F.; Boyer-Richard, S.; Le Corre, A.; Durand, O.; Guillemoles, J.-F. Quantitative experimental assessment of hot carrier-enhanced solar cells at room temperature. *Nature Energy* **2018**, *3*, 236–242.
- (55) Giteau, M.; de Moustier, E.; Suchet, D.; Esmailpour, H.; Sodabanlu, H.; Watanabe, K.; Collin, S.; Guillemoles, J.-F.; Okada, Y. Identification of surface and volume hot-carrier thermalization mechanisms in ultra-thin GaAs layers. *Journal of Applied Physics* **2020**, *128*, 193102.
- (56) Kornbluth, M.; Nitzan, A.; Seideman, T. Light-induced electronic non-equilibrium in plasmonic particles. *The Journal of Chemical Physics* **2013**, *138*, 174707.
- (57) Bebb, H. B.; Williams, E. W. In *Chapter 4 Photoluminescence I: Theory*; Willardson, R. K., Beer, A. C., Eds.; Semiconductors and Semimetals; Elsevier, 1972; Vol. 8; pp 181 – 320.
- (58) Williams, E. W.; Bebb, H. B. In *Chapter 5 Photoluminescence II: Gallium Arsenide*; Willardson, R. K., Beer, A. C., Eds.; Semiconductors and Semimetals; Elsevier, 1972; Vol. 8; pp 321 – 392.
- (59) Snoke, D. W. Density dependence of electron scattering at low density. *Phys. Rev. B* **1994**, *50*, 11583–11591.
- (60) Kash, J. A. Carrier-carrier scattering: An experimental comparison of bulk GaAs and GaAs/Al_xGa_{1-x}As quantum wells. *Phys. Rev. B* **1993**, *48*, 18336–18339.

- (61) Snoke, D. W. Theory of electron-electron scattering at low density. *Phys. Rev. B* **1993**, *47*, 13346–13352.
- (62) Becker, P. C.; Fragnito, H. L.; Cruz, C. H. B.; Fork, R. L.; Cunningham, J. E.; Henry, J. E.; Shank, C. V. Femtosecond Photon Echoes from Band-to-Band Transitions in GaAs. *Phys. Rev. Lett.* **1988**, *61*, 1647–1649.
- (63) Vurgaftman, I.; Meyer, J. R.; Ram-Mohan, L. R. Band parameters for III–V compound semiconductors and their alloys. *Journal of Applied Physics* **2001**, *89*, 5815–5875.
- (64) Strauss, U.; Rühle, W. W.; Köhler, K. Auger recombination in intrinsic GaAs. *Applied Physics Letters* **1993**, *62*, 55–57.
- (65) Govoni, M.; Marri, I.; Ossicini, S. Auger recombination in Si and GaAs semiconductors: Ab initio results. *Phys. Rev. B* **2011**, *84*, 075215.
- (66) Achermann, M.; Bartko, A. P.; Hollingsworth, J. A.; Klimov, V. I. The effect of Auger heating on intraband carrier relaxation in semiconductor quantum rods. *Nature Physics* **2006**, *2*, 557–561.
- (67) Sze, S. M. *Physics of Semiconductor Devices*; John Wiley & Sons, Ltd, 2006; pp 5–75.
- (68) Sivan, Y.; Un, I. W.; Dubi, Y. Assistance of plasmonic nanostructures to photocatalysis - just a regular heat source. *Faraday Discuss.* **2019**, *214*, 215–233.
- (69) Aspnes, D. E.; Studna, A. A. Dielectric functions and optical parameters of Si, Ge, GaP, GaAs, GaSb, InP, InAs, and InSb from 1.5 to 6.0 eV. *Phys. Rev. B* **1983**, *27*, 985–1009.
- (70) Duh, Y.-S. et al. Giant photothermal nonlinearity in a single silicon nanostructure. *Nature Communications* **2020**, *11*, 4101.
- (71) Zhang, T. et al. Anapole mediated giant photothermal nonlinearity in nanostructured silicon. *Nature Communications* **2020**, *11*, 3027.
- (72) Cognet, L.; Berciaud, S.; Lasne, D.; Lounis, B. Photothermal Methods for Single Non-luminescent Nano-Objects. *Analytical Chemistry* **2008**, *80*, 2288–2294.
- (73) Jaque, D.; Vetrone, F. Luminescence nanothermometry. *Nanoscale* **2012**, *4*, 4301–4326.
- (74) Roman, B. J.; Villegas, N. M.; Lytle, K.; Sheldon, M. Optically Cooling Cesium Lead Tribromide Nanocrystals. *Nano Letters* **2020**, *20*, 8874–8879.